

# Al<sub>2</sub>O<sub>3</sub> Modified Cr<sub>2</sub>O<sub>3</sub> Thick Film as Ethanol Gas Sensor

Dr. P.M. Chandak

Department of Physics, B.B. Arts, N.B. Commerce and B.P. Science College, Digras-445203, Maharashtra State, India

## Abstract

Chromium oxide (Cr<sub>2</sub>O<sub>3</sub>), Nanocrystalline powder, was prepared by chemical co-precipitation method. The crystallite size of Cr<sub>2</sub>O<sub>3</sub> was found to be in the range of 18 nm. Thick films of pure Cr<sub>2</sub>O<sub>3</sub> were prepared by screen-printing technique and Al<sub>2</sub>O<sub>3</sub>-surface modified Cr<sub>2</sub>O<sub>3</sub> thick films were prepared by dipping method for 4 min. The material was studied by various characterization techniques viz. XRD, SEM, EDX, etc. 4 min dipped Al<sub>2</sub>O<sub>3</sub> modified Cr<sub>2</sub>O<sub>3</sub> thick films showed highest response to ethanol (100 ppm) gas at 50°C as compare to other gases.

The effects of surface modification on the gas response, selectivity, response time and recovery time of Cr<sub>2</sub>O<sub>3</sub> based thick film gas sensor in the presence of NH<sub>3</sub>, Cl<sub>2</sub>, LPG, CO<sub>2</sub>, H<sub>2</sub>S and C<sub>2</sub>H<sub>5</sub>OH gases were studied and discussed.

**Keywords:** Cr<sub>2</sub>O<sub>3</sub>; XRD; Ethanol gas; Response time.

## 1. Introduction

Nanotechnology plays a vital role in gas sensors. In the field of gas sensing, nanomaterials have a huge potential in comparison to bulk materials. It has been observed that nanostructure and bulk structure of same material show different physical and chemical properties.

The semiconductor metal oxides based gas sensors are playing an important role in the detection of toxic pollutants and control over the industrial processes. Generally, two techniques are used for the fabrication of semiconductor metal oxide gas sensors, namely thin film [1] and thick film sensors [2]. It has been observed that, thick film gas sensors fabricated by screen-printing technique have some advantages such as simple fabrication, low price and good sensing properties over other types of gas sensors [3–5]. It has been observed that the adsorption of gas molecules on a surface of metal oxide semiconductor can cause a significant change in the electrical conductivity or resistivity of the material [6]. Moreover, the morphology, structure and chemical composition of semiconductors oxide plays an important role in determining their gas sensing properties. It has been found that, Solid state gas sensors based on transition metal oxides (TiO<sub>2</sub>, SnO<sub>2</sub>, WO<sub>3</sub>, ZnO, Cr<sub>2</sub>O<sub>3</sub> and In<sub>2</sub>O<sub>3</sub>) show fast sensing response, simple execution and low costs [7, 8].

In recent years, it has been observed that, nanostructure chromium oxide (Cr<sub>2</sub>O<sub>3</sub>) with large ratio of surface area to volume has attracted more attention [9–13]. It has been studied that Cr<sub>2</sub>O<sub>3</sub>[14–27] was considerably used as gas sensing element. The pure Cr<sub>2</sub>O<sub>3</sub> was reported as poor gas sensing element. Cr<sub>2</sub>O<sub>3</sub> is the most stable oxide among all the various oxides of chromium. P-type semiconductor shows high electrical conductivity with reasonable levels of electron transfer [28]. A semiconductor metal oxide Cr<sub>2</sub>O<sub>3</sub> is extensively used in many fields' namely catalytic reactions [29], optical coating [30], infrared sensors [31], and gas sensors [32], doping in varistors compounds [33]. The gas sensing mechanisms for p-type semiconductor metal oxide are similar to those of n-types. But in this regard less number of investigations is carried out [34]. For gas sensing applications, there are some reports based on the Cr<sub>2</sub>O<sub>3</sub> thick films for vapor sensing (e.g. ethanol) [35–39].

It well knows that; ethanol (C<sub>2</sub>H<sub>5</sub>OH) is an inflammable volatile organic compound. It is toxic in nature and also most considerably used alcohols. It is widely used in the food industries; bio-medicine and chemical industries [40]. It has been observed that exposure to ethanol vapour causes health related problems, such as breathing problems, a continuous pain in the head, sleepiness, eyes irritation, and liver damage [41]. Workers working in the ethanol synthesis industries have much chances of being victim of digestive and respiratory track cancer. Ethanol sensor play an vital role in medical, chemical and food industries and also in

environmental protection [42,43]. In the recent years, many efforts have been made to enhance the ethanol sensing performance of metal oxide sensors with high response and selectivity [44]. But, still there is a need to fabricate ethanol sensor and monitor ethanol vapors.

The aim of the present work is to fabricate the thick film sensor by activating pure  $\text{Cr}_2\text{O}_3$  thick films, to detect ethanol. The present paper reports the structure, morphology and gas sensing properties of pure and 4 min dipped modified  $\text{Cr}_2\text{O}_3$  based thick films.

## 2. Experimental Details

### 2.1. Preparation of Nanocrystalline $\text{Cr}_2\text{O}_3$ Powders

All chemicals used in the synthesis process were of analytical grade. Nanocrystalline  $\text{Cr}_2\text{O}_3$  powders were synthesized by chemical precipitation method. The details regarding preparation of nanocrystalline  $\text{Cr}_2\text{O}_3$  was already published in our earlier publication [45]. The synthesized nanocrystalline  $\text{Cr}_2\text{O}_3$  powders were used for further study.

### 2.2. Preparation of thick films

Thick films of nanocrystalline  $\text{Cr}_2\text{O}_3$  Powders were prepared by using screen printing technique. The details regarding preparation of pure  $\text{Cr}_2\text{O}_3$  thick films were already published in our earlier publication [45].

### 2.3. $\text{Al}_2\text{O}_3$ modified $\text{Cr}_2\text{O}_3$ thick films

Surface of pure  $\text{Cr}_2\text{O}_3$  thick films were modified by dipping them into 0.01M aqueous solution of  $\text{AlCl}_3$  (99% AR grade, Merck) for 4 min. Dipped thick films were dried under IR lamp for 1 h. Dried thick films were fired at  $500^\circ\text{C}$  for 30 min. The  $\text{AlCl}_3$  dispersed on the film surface was oxidised to  $\text{Al}_2\text{O}_3$  in firing process and sensor element with different mass % of  $\text{Al}_2\text{O}_3$  on the surface of  $\text{Cr}_2\text{O}_3$  thick film was obtained. This surface modified thick film is called as 4 min dipped  $\text{Al}_2\text{O}_3$  modified  $\text{Cr}_2\text{O}_3$  thick film.

### 3.1 Thickness measurement

'Marutek film Thickness Measurement System' technique was used for measurement of thickness of pure  $\text{Cr}_2\text{O}_3$  and  $\text{Al}_2\text{O}_3$  modified  $\text{Cr}_2\text{O}_3$  thick films with the help of provided equipment. The thickness of all films was observed in the range from 32 to 36  $\mu\text{m}$ . Thick films of nearly uniform thickness were used for further characterization and gas sensing purpose.

### 3.2. X-ray diffraction

The crystallographic structure of the synthesized  $\text{Cr}_2\text{O}_3$  nanostructure was characterized by powder x-ray diffraction. The details regarding X-ray diffraction of nanocrystalline  $\text{Cr}_2\text{O}_3$  powders was already published in our earlier publication [45].

### 3.3 Scanning electron microscopy

Fig. 2 (a-b) depicts FE-SEM images of the pure and 4 min dipped  $\text{Al}_2\text{O}_3$  modified  $\text{Cr}_2\text{O}_3$  thick films prepared by screen printing technique. Fig. 2(a) shows the FE-SEM image of the pure  $\text{Cr}_2\text{O}_3$  film. The pure  $\text{Cr}_2\text{O}_3$  film consists of randomly distributed grains with smaller size and shape distribution. The average size of  $\text{Cr}_2\text{O}_3$  grains are approximately 29 nm to 44 nm. Fig. 2 (b) depicts the microstructure of  $\text{Al}_2\text{O}_3$  modified  $\text{Cr}_2\text{O}_3$  thick film for 4 min dipping. It is observed from this figure that the dipping of  $\text{Al}_2\text{O}_3$  affected the microstructure of  $\text{Cr}_2\text{O}_3$ . It consists of large number of nearly similar sized grains of  $\text{Al}_2\text{O}_3$  fitted with the comparable sized grains of  $\text{Cr}_2\text{O}_3$ . The film consists of grains with sizes ranging from 26 nm to 41 nm, distributed non-uniformly. These grains could be attributed to  $\text{Al}_2\text{O}_3$ . Due to such deposition of grains, surface to volume ratio of  $\text{Al}_2\text{O}_3$  modified  $\text{Cr}_2\text{O}_3$  thick films may be increased.

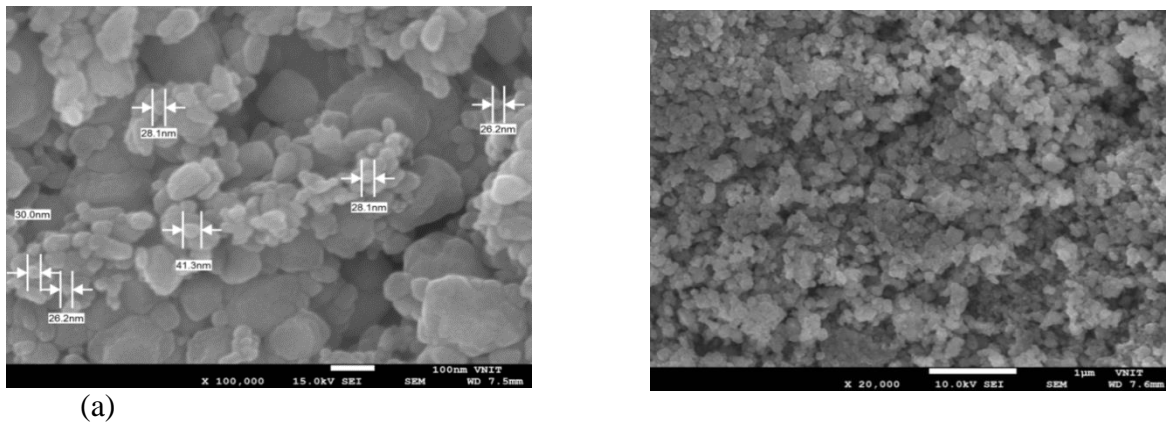
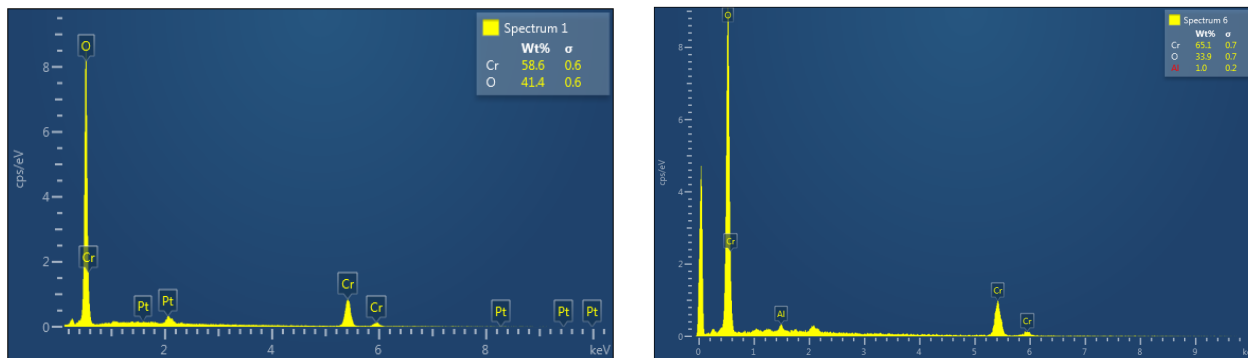


Fig. 2: FE-SEM images for (a) pure  $Cr_2O_3$  nanoparticles (b)  $Al_2O_3$  modified  $Cr_2O_3$  thick film (4 min dip.)

### 3.4 Quantitative Elemental Analysis (EDX)

The quantitative elemental composition of the pure and  $Al_2O_3$  modified  $Cr_2O_3$  thick films were analyzed by using an Energy Dispersive Spectrometer (EDS). Fig.3 (a-b) represents the EDS patterns of pure and 4 min dipped  $Al_2O_3$  modified  $Cr_2O_3$  thick films. The EDS analysis proved the presence of Cr, Al and O in the  $Al_2O_3$  modified  $Cr_2O_3$  thick films and no other impurity elements were present in the  $Al_2O_3$  modified  $Cr_2O_3$  thick films. The synthesized powder of pure  $Cr_2O_3$  is excess in oxygen. Excess or deficiency of the constituent element proved the semiconducting nature of the material. Hence pure  $Cr_2O_3$  is semiconducting in nature. Also, the mass % of Cr and O in modified sample is not as per the stoichiometric proportion and the sample is observed to be oxygen deficient or excess in chromium. Thus, the maximum numbers of electrons are free for current and they behave as the majority charge carriers. Table 3.1 shows quantitative elemental analysis of pure  $Cr_2O_3$  and 4 min dipped  $Al_2O_3$  modified  $Cr_2O_3$  thick films.

Also the results of EDS analysis confirmed that only Cr, O and Al are present in surface modified thick film sample and no impurity elements were present in pure and modified samples.



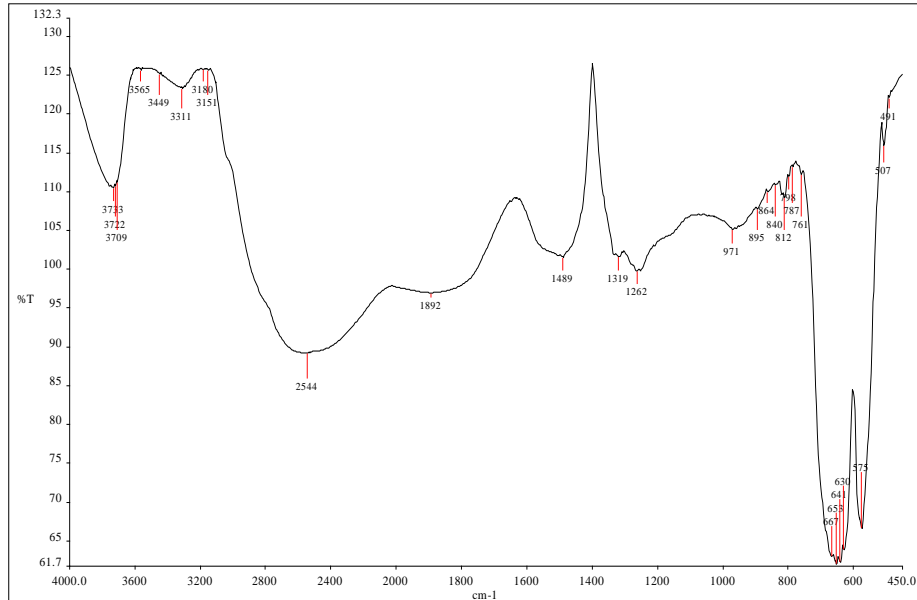
patterns for a) pure  $Cr_2O_3$  thick film b)  $Al_2O_3$  modified  $Cr_2O_3$  thick film (4 min dip.)

Table 3.1: Mass % of Cr, O and Al elements in pure and modified thick films

Element	Pure $Cr_2O_3$	4 min dipped $Al_2O_3$ modified $Cr_2O_3$ thick films
O	41.4	33.9
Cr	58.6	65.1
Al	—	1.0

### 3.5 Fourier Transform infrared (FT-IR)

FT-IR spectroscopy was used to obtain the structural information of the materials. Fig.4 depicts FT-IR spectrum of  $\text{Cr}_2\text{O}_3$ . In IR analysis the vibrations of ions in the crystal lattice are generally observed in the range of  $4000 - 450 \text{ cm}^{-1}$ . All the observed peaks are in well agreement with the standard reported results. High intensity of the peaks of  $\text{Cr}_2\text{O}_3$  bands proved the good crystalline nature of the materials [46].



**Fig.4: FT-IR spectrum of  $\text{Cr}_2\text{O}_3$**

### 3.6. I-V characteristics of pure and 4 min dipped $\text{Al}_2\text{O}_3$ modified $\text{Cr}_2\text{O}_3$ thick films

Fig.5 depicts the I-V characteristics of pure and 4 min dipped  $\text{Al}_2\text{O}_3$  modified  $\text{Cr}_2\text{O}_3$  thick films. The bias voltage was increased in the step of 5V from 0 to 30 V and corresponding current was recorded. The measurement was repeated with negative voltage. The nature of the I-V characteristics curves for given samples showed that the contacts are ohmic in nature.

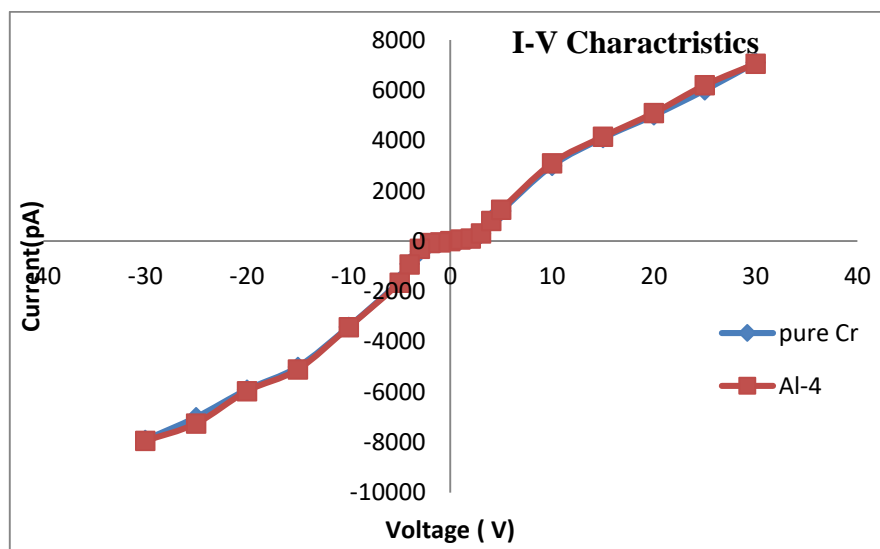


**Fig.6: I-V Characteristics of pure and 4min dipped  $\text{Al}_2\text{O}_3$  modified  $\text{Cr}_2\text{O}_3$  thick films at room temperature.**

### 3.7 Gas sensing performance of sensor

### 3.7.1 Gas Sensing Performance of pure and Al<sub>2</sub>O<sub>3</sub> modified Cr<sub>2</sub>O<sub>3</sub> thick films

Fig.6 depicts the gas response of pure and Al<sub>2</sub>O<sub>3</sub> modified Cr<sub>2</sub>O<sub>3</sub> thick films versus operating temperature. At operating temperatures changing from room temperature to 400°C, the gas response to 100 ppm ethanol by pure and Al<sub>2</sub>O<sub>3</sub> modified Cr<sub>2</sub>O<sub>3</sub> thick films were investigated and studied.

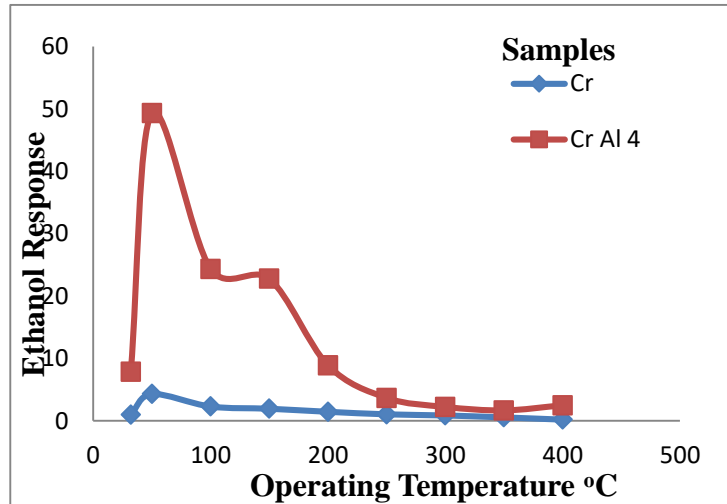


**Fig. 6: Variation of gas response of pure and Al<sub>2</sub>O<sub>3</sub> modified Cr<sub>2</sub>O<sub>3</sub> thick films with operating temperature.**

Fig. 6 also shows the variation of gas response to 100 ppm ethanol gas by a pure Cr<sub>2</sub>O<sub>3</sub> thick film with changing operating temperature from room temperature to 400°C. The response to ethanol gas goes on increasing with increase of operating temperature upto 50°C and then decreases with the further increase of operating temperature. As we know that, response to an ethanol gas is generally depends on the number of oxygen ions adsorbed on the surface of the film with a target gas. If the film surface chemistry was favourable for adsorption, response and selectivity would be enhanced. The pure Cr<sub>2</sub>O<sub>3</sub> thick film showed poor response to ethanol gas, as oxygen adsorption seems to be poor. So, to enhance the gas sensing performance of pure Cr<sub>2</sub>O<sub>3</sub>, it is essential to modify pure Cr<sub>2</sub>O<sub>3</sub>.

It is also observed from figure that 4min dipped Al<sub>2</sub>O<sub>3</sub> modified Cr<sub>2</sub>O<sub>3</sub> thick film gives highest response to 100 ppm ethanol at 50°C as compared to pure Cr<sub>2</sub>O<sub>3</sub> thick film. It showed the highest response (49.32) to 100 ppm ethanol vapors at 50°C. The highest response may be attributed due to the optimal number of Al<sub>2</sub>O<sub>3</sub> grains spread over the surface. So, more amount of oxygen would adsorb on surface and oxidation of target gas would be more giving larger response.

### 3.7.2 Selectivity

Fig. 7 depicts the selectivity of all, pure and 4 min dipped Al<sub>2</sub>O<sub>3</sub> modified Cr<sub>2</sub>O<sub>3</sub> thick films for 100 ppm concentration of LPG, C<sub>2</sub>H<sub>5</sub>OH, CO<sub>2</sub>, NH<sub>3</sub>, H<sub>2</sub>S and H<sub>2</sub> at 50°C. The pure and 4 min dipped Al<sub>2</sub>O<sub>3</sub> modified Cr<sub>2</sub>O<sub>3</sub> thick films show higher selectivity for C<sub>2</sub>H<sub>5</sub>OH gas among all the gases. It is clear from figure that the 4 min dipped Al<sub>2</sub>O<sub>3</sub> modified Cr<sub>2</sub>O<sub>3</sub> thick film showed highest selectivity for ethanol gas at 50°C as compared to all other tested gases: LPG, CO<sub>2</sub>, NH<sub>3</sub>, H<sub>2</sub> and H<sub>2</sub>S.



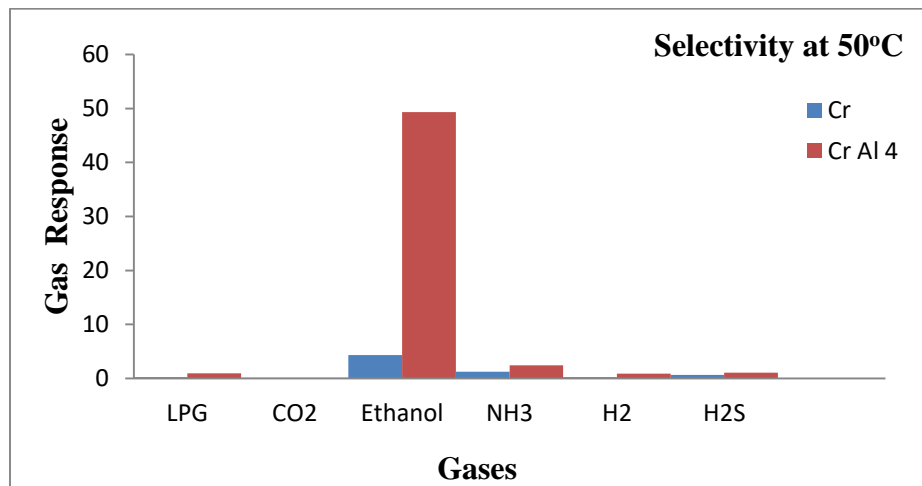


Fig. 7: Selectivity of pure and 4 min dipped Al<sub>2</sub>O<sub>3</sub> modified Cr<sub>2</sub>O<sub>3</sub> thick films

### 3.7.3 Active Nature

Fig. 8 exhibits the relation between ethanol gas response of pure and 4 min dipped Al<sub>2</sub>O<sub>3</sub> modified Cr<sub>2</sub>O<sub>3</sub> thick films with the different concentration of C<sub>2</sub>H<sub>5</sub>OH gas at 50°C. It is observed from the figure that the gas response of 4 min dipped Al<sub>2</sub>O<sub>3</sub> modified Cr<sub>2</sub>O<sub>3</sub> thick film increases linearly with ethanol gas concentration up to 100 ppm. The rate of increase in response was relatively larger and linear up to 100 ppm and saturated beyond 100 ppm. So, the active region for the ethanol sensor is up to 100 ppm. At the higher gas concentrations, there would be multilayer of gas molecules on the film surface resulting in saturation in gas response beyond 100 ppm gas.

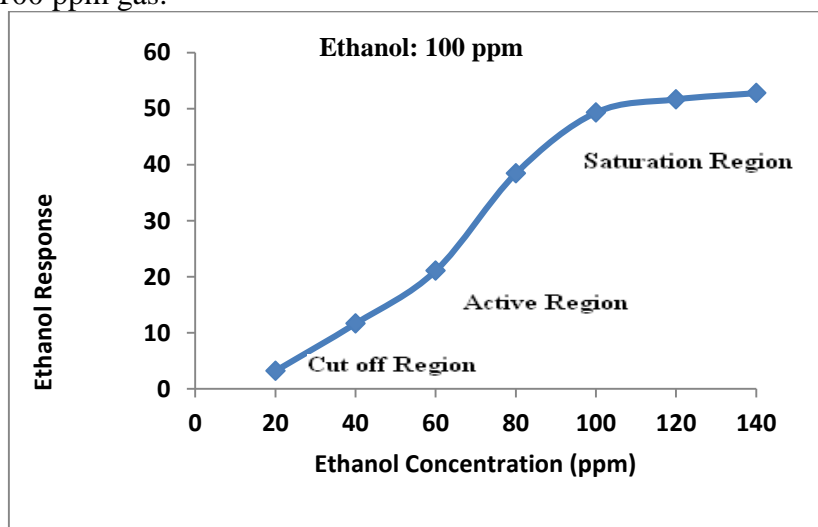


Fig. 8: Variation of ethanol response with ethanol concentration (ppm)

### 3.7.4 Response and Recovery time

The response and recovery time of the 4 min dipped Al<sub>2</sub>O<sub>3</sub> modified Cr<sub>2</sub>O<sub>3</sub> thick film to 100 ppm of ethanol are 12 s and 20 s respectively. Thus the sensor showed very instant response and rapid recovery time to ethanol gas. For better performance of the sensor the recovery should be very fast. This is the main and important feature of this sensor.

### 3.7.5 Stability

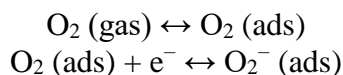
The ethanol gas response of 4 min dipped Al<sub>2</sub>O<sub>3</sub> modified Cr<sub>2</sub>O<sub>3</sub> thick film sensor for 100 ppm at 50°C was constantly measured for 80 days in the interval of 10 days. It has been observed that a sensor showed a very stable response over 80 days, confirming the stability and reproducibility of the sensor.

### 3.7.6 Ethanol gas sensing mechanism

The semiconductor metal oxide thick film gas sensor works on the principle of change in electronic conductivity or resistivity of thick film on exposure to ethanol gas. In the gas sensing mechanism the change in resistance is caused by the adsorption and desorption of gas molecules on the surface of the thick films.

When ethanol gas molecules react with surface of metal oxide gas sensor, transfer of electrons between them takes place.

As we know that, oxygen is the second largest element in the atmosphere after nitrogen. So, oxygen plays a prime role in the adsorption process due to its strong electronegativity and lone pairs of electrons. When semiconducting gas sensor is exposed to air, oxygen molecules easily get adsorbed on the surface of the sensor. During adsorption process the oxygen molecules gains an electron from the thick film surface and changed into ionic form such as  $O_2^-$ ,  $O^-$  and  $O^{2-}$  which capture electrons from the conduction band. The reaction kinetics is as follows [47]:



This results in decreasing electronic conductivity of the film. During gas sensing mechanism, the molecules of ethanol gas get oxidised with ionic form of oxygen to form  $CO_2$  and  $H_2O$  with release of energy. This released energy is sufficient for trapped electrons to jump back into the conduction band of modified  $Cr_2O_3$ . Thus there is a decrease in resistance of the sensor and hence, increase in conductivity of the sensor.

#### 4 Conclusions:

The obtained results can be summarised as below.

1. Pure  $Cr_2O_3$  thick films are less conductive as compared to 4 min dipped  $Al_2O_3$  modified  $Cr_2O_3$  thick film.
2. A pure  $Cr_2O_3$  thick film showed poor gas response to all tested reducing gas.
3.  $Al_2O_3$  modified  $Cr_2O_3$  thick film (4 min dip) showed higher gas response to 100 ppm of ethanol gas as compared to pure  $Cr_2O_3$  thick film.
4. The  $Al_2O_3$  modified  $Cr_2O_3$  thick film sensor showed good selectivity to ethanol gas against  $H_2$ , LPG,  $CO_2$ ,  $H_2S$  and  $NH_3$  gases at  $50^\circ C$ .
5.  $Al_2O_3$  modified  $Cr_2O_3$  thick film (4 min dip) shows fast response (12 s) and rapid recovery (20 s).

#### References

1. M. Mabrook, P. Hawkins, Sens. Actuators B 75 (2001)197–202.
2. U.-S. Choi, G. Sakai, K. Shimanoe, N. Yamazoe, Sens. Actuators B 98 (2004)166–173.
3. W. Noh, Y. Shin, J. Kim, W. Lee, K. Hong, S.A. Akbar, J. Park, Solid State Ionics 152–153 (2002) 827–832.
4. M.C.Carotta,G.Martenelli, Y. Sadaoka, P. Nunziante, E. Traversa, Sens.Actuators B 48 (1998) 270–276.
5. V. Guidi, M.A. Butturi, M.C. Carotta, B. Cavicchi, M. Ferroni, C. Malagu,G. Marinelli, D. Vincenzi, M. Sacerdoti, M. Zen, Sens. Actuators B 84 (2002) 72–77.
6. Choi J.Y.,Oh T. S., Thin Solid Films 547 (2013) 230-234.
7. H. Meixner, J. Gerblinger, U. Lampe, M. Fleischer, Sensors and Actuators B 23, 119-125, (1995).
8. J.T. Woetsman, E. M. Logothetis, the Industrial Physicist 20-24, Ed. American Institute of Physics, (1995).
9. S.M. El-Sheikh, R.M. Mohamed, O.A. Fouad, Journal of Alloys and Compounds 482 (2009) 302–307.
10. H. Xu, T. Lou, Y. Li, Inorganic Chemistry Communications 7 (2004) 666–668.
11. R.C. Ku, W.L. Winterbottom, Thin Solid Films 127 (1985) 241–256.
12. A. Cellard, V. Garnier, G. Fantozzi, G. Baret, P. Fort, Ceramics International 35(2009) 913–916.
13. S. Pokhrel, K.S. Nagaraja, Sensors and Actuators B 92 (2003) 144–150.
14. T. Jantson, T. Avarmaa, H. Mandar, T. Uustave, R. Jaaniso, Sens. Actuators B 109 (2005) 24-31.
15. L. P. Martin, A. Q. Pham, R. S. Glass, Sens. Actuators B 96 (2003) 53-60.
16. A. M. Ruiz, G. Sakai, A. Cornet, K. Shimanoe, J. R. Morante, N. Yamazoe, Sens. Actuators B 93 (2003) 509-518.
17. Y. Li, W. Wlodarski, K. Galatsis, S. Moslih, J. Cole, S. Russa, N. Rockelmann, Sens. Actuators B 83 (2002) 160-163.
18. V. Jayaraman, K. Gnanasekar, E. Prabhu, T. Gnanasekaran, G. Periaswmi, Sens. Actuators B 55 (1999) 175-179.

19. F. Lin, Y. Takao, Y. Shimizu, M. Egashira, *Sens. Actuators B* 25 (1995) 843-850.
20. B. K. Miremadi, R. C. Singh, Z. Chen, S. R. Morrison, K. Colbow, *Sens. Actuators B* 21 (1994) 1-4.
21. D. Baresel, W. Gellert, W. Sarholz, P Scharner, *Sens. Actuators B* 6 (1984) 35-50.
22. P. T. Moseley, D. E. Williams, *Sens. Actuators B* 1 (1990) 113-115.
23. A. Gurlo, N. Barsan, U. Weimar, Y. Shimizu, *The 10<sup>th</sup> international meeting on chemical sensors, Tsukuba, Japan, (2004)* 152-153.
24. Y. Takao, Y. Shimizu, M. Egashira, *Digest of 9<sup>th</sup> chemical sensor symposium, Aoyama Gakuin University, (1989)* 29.
25. M. Kadosaki, K. Tanimoto, C. Tatsuyama, K. Komori, S. Taniguchi, *proceedings of 32<sup>nd</sup> chemical sensor symposium, 17 (2001)* A8.
26. C. Cantalini, *J. European ceramic soc.* 24 (2004) 1421-1424.
27. L. Mancic, Z. Marinkovic, P. Vulic, C. Moral, O. Milosevic, *Sensors* 3 (2003) 415-423.
28. Z. Pei, H. Xu, Y. Zhang, *J. Alloys Compd.* 468(2009)L5-L8.
29. J. Soldat, G.W. Busser, M. Muhler, M. Wark, *ChemCatChem* 8 (2016) 153-156.
30. N.G. Semaltianos, J.M. Friedt, R. Chassagnon, V. Moutarlier, V. Blondeau-Patissier, G. Combe, M. Assoul, G. Monteil, *J. Appl. Phys.* 119 (2016)204903-2049010.
31. C.H. Bu, G. He, J.K. Ye, Y. Li, J.X. Liu, J.T. Li, *J. Ceram. Soc. Jpn.* 124 (2016)768-773.
32. S. Park, G.-J. Sun, C. Jin, H.W. Kim, S. Lee, C. Lee, *ACS Appl. Mater. Interfaces* 8 (2016) 2805-2811.
33. Shahraki MM, Shojaee SA, Sani MAF, Nemati A, Safaee I. *Solid State Ion* 190 (2011) 99-105.
34. D.K. Aswal, S.K. Gupta (Eds.), *Science and Technology of Chemiresistor Gas Sensors*, Nova Science Publisher, NY, USA, 2007.
35. C. Cantalini, *J. Eur. Chem. Soc.* 24 (2004) 1421-1424.
36. D.N. Suyavanshi, D.R. Patil, L.A. Patil, *Sens. Actuators B: Chem.* 134 (2008) 579-584.
37. J. Yoo, Eric D. Wachsman, *Sens. Actuators B: Chem.* 123 (2007) 915-921.
38. D.R. Patil, L.A. Patil, P.P. Patil, *Sens. Actuators B: Chem.* 126(2007) 368-374.
39. D.R. Patil, L.A. Patil, *Talanta* 77 (2009) 1409-1414.
40. S.G. Leonardi, A. Mirzaei, A. Bonavita, S. Santangelo, P. Frontera, F. Pantò, P.L. Antonucci, G. Neri, *Nanotechnology* 27 (2016) 075502.
41. A. Mirzaei, S. Park, G.J. Sun, H. Kheel, C. Lee, S. Lee, *J. Korean Phys. Soc.* 69 (2016) 373-380.
42. N. Hu, Y. Wang, J. Chai, R. Gao, Z. Yang, E.S.W. Kong, Y. Zhang, *Sens. Actuators B* 163(2012) 107-114.
43. Y. Lei, W. Chen, A. Mulchandani, *Anal. Chim. Acta* 568(2006) 200-210.
44. A. Boudiba, C. Zhang, C. Navio, C. Bittencourt, R. Snyders, M. Debliquy, *Procedia Eng.* 5 (2010) 180-183
45. P.M. Chandak, F.C. Raghuwanshi, V.D. Kapse, V.S. Kalyamwar, *Int. Res. J. of Science & Engineering*, 2018; Vol. 6 (6): 221-230.
46. M. Abdullah, F. Rajab and S. Al-Abbas, *AIP Advances*, 4, 027121 (2014), 1-11.
47. A. Mirzaei, S. Park, H. Kheel, G.-J. Sun, S. Lee, C. Lee, *Ceram. Interface* 42 (2016) 6187-6197.